

The hot γ Doradus and Maia stars

L. A. Balona¹, C. A. Engelbrecht², Y. C. Joshi³, S. Joshi³, K. Sharma⁴, E. Semenko⁵, G. Pandey⁶, N. K. Chakradhari⁷, David Mkrtichian⁸, B. P. Hema⁶, J. M. Nemeč⁹

¹South African Astronomical Observatory, P.O. Box 9, Observatory 7935, South Africa, lab@sao.ac.za

²Department of Physics, University of Johannesburg, PO Box 524, Auckland Park, Johannesburg 2006, South Africa

³Aryabhata Research Institute of Observational Sciences (ARIES), Manora peak, Nainital, India

⁴Department of Physics and Astrophysics, University of Delhi, Delhi - 110007, India

⁵Special Astrophysical Observatory, Russian Academy of Sciences, Nizhny Arkhyz, 369167, Russia sea@sao.ru

⁶Indian Institute of Astrophysics, Bengaluru, Karnataka 560034, India

⁷School of Studies in Physics and Astrophysics, Pt Ravishankar Shukla University, Raipur 492 010, India

⁸National Astronomical Research Institute of Thailand, 191 Huay Kaew Road, Muang, 50200, Chiangmai, Thailand

⁹Department of Physics & Astronomy, Camosun College, Victoria, British Columbia, V8P 5J2, Canada

ABSTRACT

The hot γ Doradus stars have multiple low frequencies characteristic of γ Dor or SPB variables, but are located between the red edge of the SPB and the blue edge of the γ Dor instability strips where all low-frequency modes are stable in current models of these stars. Though δ Sct stars also have low frequencies, there is no sign of high frequencies in hot γ Dor stars. We obtained spectra to refine the locations of some of these stars in the H-R diagram and conclude that these are, indeed, anomalous pulsating stars. The Maia variables have multiple high frequencies characteristic of β Cep and δ Sct stars, but lie between the red edge of the β Cep and the blue edge of the δ Sct instability strips. We compile a list of all Maia candidates and obtain spectra of two of these stars. Again, it seems likely that these are anomalous pulsating stars which are currently not understood.

Key words: stars: oscillations – stars: variables: general

1 INTRODUCTION

The γ Doradus variables are early F or late A stars which lie on or just above the main sequence and which vary in light with multiple frequencies in the range 0.3–5.0 d⁻¹. The prototype of the class was discovered to be variable by Cousins & Warren (1963) and subsequently recognized as a new class of pulsating star by Balona et al. (1994). There are over 60 known γ Dor stars discovered by ground-based observations (Handler 1999; Henry & Fekel 2005; Henry et al. 2005; De Cat et al. 2006). Many hundreds more γ Dor stars have been discovered with the *Kepler* satellite (Balona et al. 2011a; Bradley et al. 2015).

The closely related δ Scuti variables are A–F stars which pulsate with multiple frequencies as high as 100 d⁻¹, but also include the low frequencies found in γ Dor stars. Ground based observations are not sufficiently precise to detect these low frequencies, which is why δ Sct stars were originally thought to pulsate only in high-frequency modes, typically with frequencies $\nu > 5$ d⁻¹. Observations from space using the *Kepler* satellite show that, in fact, all δ Sct stars contain low frequencies (Balona 2014). The low frequencies reach maximum amplitudes in the region overlapping the blue edge of the γ Dor instability strip. From the ground, δ Sct

stars with both high and low frequencies, the “ γ Dor/ δ Sct hybrids”, are mostly seen in this region of the H-R diagram. This term arises from a misconception since low frequencies are nearly always detected in δ Sct stars given sufficient precision.

Whereas δ Sct stars contain both low and high frequencies, we define a γ Dor star by the presence of low frequencies and the absence of high frequencies. Pulsation in γ Dor stars is driven by the convective blocking mechanism (Guzik et al. 2000). Since this requires a convective envelope of sufficient depth, this mechanism cannot operate in stars hotter than late A or early F. The high-frequency pulsations in δ Sct stars are driven by the κ (opacity) mechanism operating in the HeII ionization zone (Pamyatnykh 2000). Models of non-rotating δ Sct stars indicate that only modes with frequencies higher than about 5 d⁻¹ are driven. The mechanism driving the low frequencies is currently not understood (Balona et al. 2015b).

The location of *Kepler* γ Dor stars in the H-R diagram was investigated by Balona et al. (2011a). The blue edge of this sample of stars is well defined and agrees with the predictions of the convective blocking mechanism. It should be noted, however, that is often impossible to distinguish between pulsation and rotation for stars with only a few close

peaks, and the sample is certainly contaminated with many non-pulsating spotted stars. It is thought that most cool stars, either fully convective or with a convective envelope like the Sun, will have spots on their surfaces. Over 500 stars of spectral types F–M are classified as rotational variables of this type (Strassmeier 2009).

While the vast majority of γ Dor stars observed by *Kepler* are cooler than the granulation boundary (the division between stars with convective and radiative envelopes), as expected, there are a few anomalous stars observed by *Kepler* which have multiple low frequencies and no detectable high frequencies, but seem to be significantly hotter than the blue edge of the γ Dor instability strip. These hot γ Dor-like stars are discussed in Balona (2014). Note that Bradley et al. (2015) analysed a large number of faint *Kepler* targets and also found a few hot γ Dor candidates.

The presence of anomalous hot γ Dor variables clearly poses a problem as there is no known mechanism to drive these pulsations. The effective temperatures, T_{eff} , are derived from multiband Sloan photometry and listed in the *Kepler Input Catalogue* (KIC, Brown et al. 2011). However, the KIC photometry does not include measurements in the UV and the derived T_{eff} are not reliable for B-type stars. It is possible that the T_{eff} for anomalous hot γ Dor stars are in error. They could, in fact, be normal γ Dor stars or SPB stars. The SPB variables are mid- to late-B stars which pulsate in multiple low frequencies driven by the κ mechanism due to the opacity bump of iron-group elements. Their light curves closely resemble those of γ Dor stars.

The cool edge of the SPB instability strip is at about 11500 K and the hot edge of the δ Sct instability strip is at about 8500 K. Between these two instability strips no pulsating star is expected to be found. However, there have been persistent reports of stars with high frequencies, typical of SPB or δ Sct variables, located in this region of the H-R diagram and termed “Maia variables”. Mowlavi et al. (2013) have found what appears to be several examples of this class in photometric observations of the young open cluster NGC 3766. They discovered a large population (36 stars) of new variable stars between the red edge of the SPB instability strip and the blue edge of the δ Sct instability strip. Most stars have periods in the range 0.1–0.7 d, with amplitudes between 1–4 mmag. About 20 percent of stars in this region of the H-R diagram were found to be variable. More recently, Balona et al. (2015a) have re-analysed the *Kepler* B stars and found many stars with well-determined T_{eff} in this region of the H-R diagram.

Apart from the low frequencies in δ Sct stars, the hot γ Dor stars and the Maia variables provide clear challenges to our current understanding of stellar pulsation. The aim of this paper is to report and analyse new spectroscopic observations of some of these stars in the *Kepler* field. Our aim is to determine whether or not the effective temperatures of these stars are in error and to decide whether they may possibly be explained as composite stars.

2 SPECTROSCOPIC OBSERVATIONS

Spectra for three stars, KIC 4281581, KIC 5113797 and KIC 8489712, were obtained in 2014 March at the Special Astrophysical Observatory (SAO) of the Russian Academy

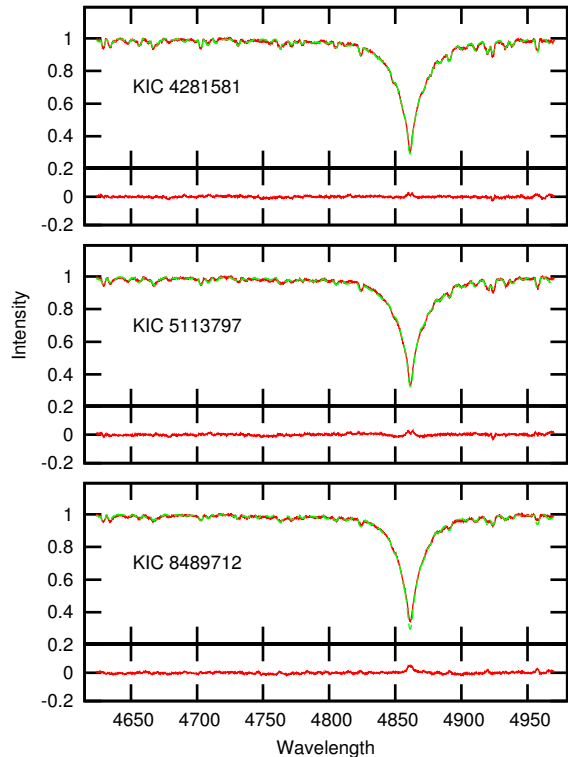


Figure 1. Observed and fitted spectra in the vicinity of $H\beta$ for three stars observed at SAO. The continuum intensity has been normalized to unity.

of Sciences with the MSS spectrograph attached to the 6-m telescope (BTA). The detector is a $2K \times 4K$ CCD. The spectra cover the wavelength range 4430–4985 Å with $R = 14000$.

The analysis was carried out in a semi-automatic manner with the latest version of SME (Valenti & Piskunov 1996). It is sometimes difficult to find a suitable fit to the core of the hydrogen line profiles, which is quite sensitive to the effective temperature and the projected rotational velocity. Observed and fitted spectra of these stars are shown in Fig. 1.

Low resolution spectra were obtained on 2015 September 23–24 with the Himalaya Faint Object Spectrograph and Camera (HFOSC) mounted on the 2.0-m Himalayan Chandra Telescope (HCT) operated by the Indian Institute of Astrophysics (IIA), Bangalore. The detector is a $2K \times 2K$ SITE CCD. Most of the spectra cover the wavelength range 3800–7000 Å with a spectral resolution $R = 1300$. A few spectra were obtained in the wavelength region 5800–8350 Å with $R = 2190$.

The spectra were analysed using ULySS (University of Lyon spectroscopic software, Koleva et al. 2009) which can also be used for the determination of the stellar atmospheric parameters. A series of modelled spectra is generated based on an empirical library and compared with the observed spectrum. The sum of the squares of the differences between the observed and modelled spectrum is minimized to obtain the best fitting parameters. The selection of the empirical library depends upon the coverage of the stellar parameters and the spectral resolution. For our analysis, the MILES interpolator (Prugniel et al. 2011), based on the MILES library

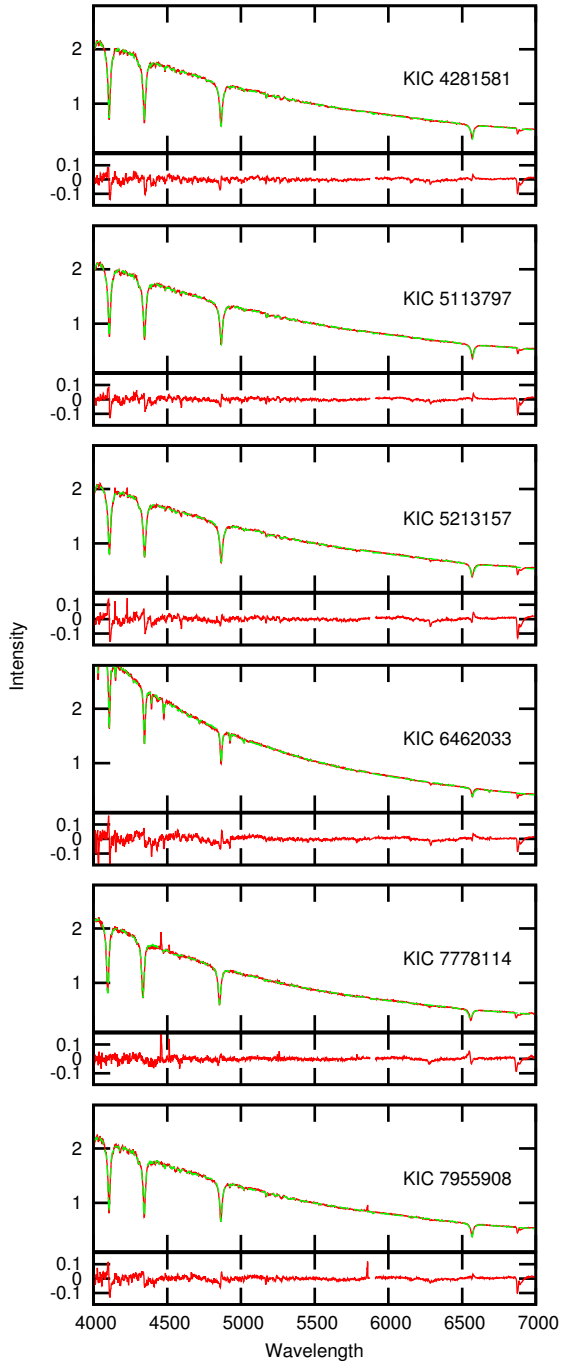


Figure 2. Observed and fitted spectra (top panel) and residuals (bottom panel) for stars observed with HFOSC. The intensity is in arbitrary units.

(Sánchez-Blázquez et al. 2006) was used. The resolution of the MILES spectra, $R \approx 2000$, closely matches with that of the spectra obtained with HFOSC at HCT. The observed and fitted spectra are shown in Figs. 2 and 3.

The derived stellar parameters are listed in Table 1 for those stars that we classified as anomalous hot γ Dor stars and in Table 2 for stars which could be assigned normal variability types, either SPB or δ Sct.

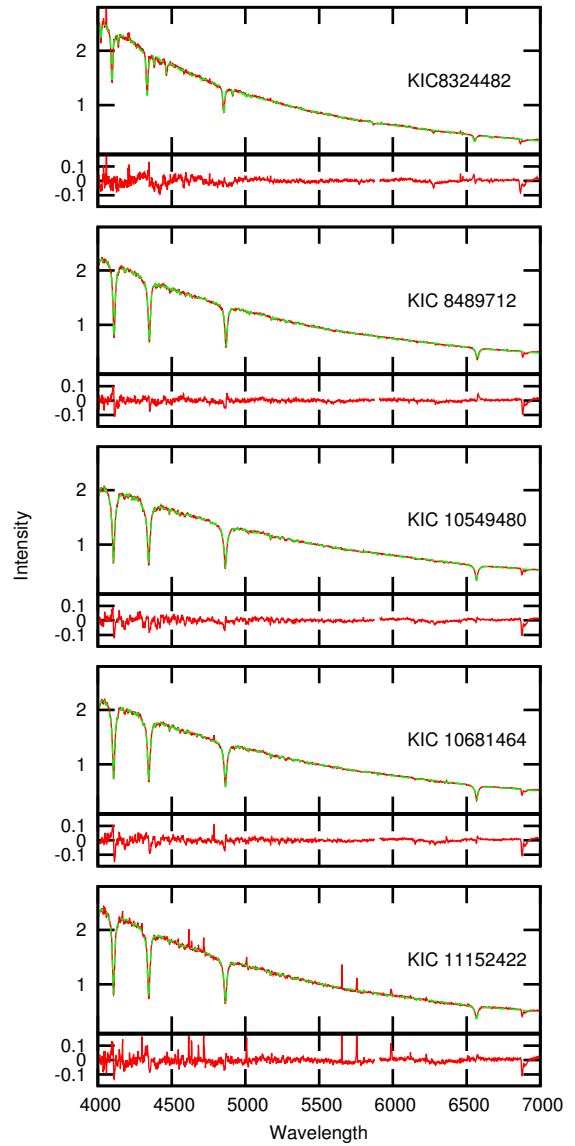


Figure 3. Observed and fitted spectra (top panel) and residuals (bottom panel) for stars observed with HFOSC.

3 STELLAR PARAMETERS

It should be noted that the KIC effective temperatures for A stars are remarkably consistent with those derived from high-dispersion spectroscopy. From 107 stars with both KIC and spectroscopic parameters, Balona et al. (2015b) found that spectroscopic estimates of T_{eff} of A stars are systematically 144 K higher than those in the KIC (the corrected KIC values are shown in Tables 1 and 2). Moreover, the standard deviation for T_{eff} is 150 K from spectroscopy and 200 K for the KIC value. The KIC effective temperature is thus quite sufficient to distinguish between normal γ Dor stars and hot γ Dor variables. However, there is a problem with the KIC value of T_{eff} for the B stars. B stars can easily be assigned temperatures within the A star region. What is required is simply to distinguish between an A star and a B star, and this is easily done with low-dispersion spectra by looking for the presence of He I lines.

Table 1. List of hot γ Doradus stars. The spectral type is taken from the literature. The *Kepler* magnitude, Kp, the corrected effective temperature, T_{eff}^1 , and surface gravity, $\log g^1$, are from the KIC. The values of T_{eff} , $\log g$, [Fe/H] and projected rotational velocity, $v \sin i$, are derived from spectra. The source of the spectroscopic stellar parameters is given in the Ref column as follows: 1 - MSS data; 2 - HFOSC data; 3 - Niemczura et al. (2015); 4 - Tkachenko et al. (2013); 5 - Ulusoy et al. (2014); 6 - Antonello et al. (2006); 7 - McDonald et al. (2012); no reference - KIC photometric values. The luminosity, $\log L/L_{\odot}$, is derived using Torres et al. (2010). Possible rotation periods, derived from the light curve, are given. The references for these periods are: a - Nielsen et al. (2013); b - Reinhold et al. (2013); c - Balona (2013).

KIC	Sp. type	Kp mag	T_{eff}^1 K	$\log g^1$ dex	T_{eff} K	$\log g$ dex	[Fe/H] dex	$v \sin i$ km s $^{-1}$	Ref	$\log \frac{L}{L_{\odot}}$	Period d
4934767		11.24	9870	4.25						1.44	
5113797		9.15	8280	3.83	7710	3.5	-0.3	137	1	1.83	2.418 ^a
					8700	4.5	-0.4		2	0.90	
	A3IV-V				8100	4.0		112	3		
5213157		11.94	8460	3.81	8700	4.5	-0.3		2	0.90	0.5452 ^b
5429163	A5V	9.72	8220	4.02	8100	4.0	-0.1	163	3	1.31	
7694191		10.78	8000	3.54						1.83	0.3762 ^c
7767565	Am	9.32			7800	3.8	0.4	65	3	1.51	
7778114		11.98	8890	4.11	9500	4.1	-0.5		2	1.50	
8489712	A2IVs	8.62	8490	3.52	8150	3.0	-0.3	120	1	2.60	
					8650	3.4	-0.7		2	2.20	
					8800	3.5	0.1	126	3		
					8270	2.9	-0.6	119	4		
8523871		12.36	8390	4.45						0.84	
10096499	A3V	6.92	7920	4.13	7960	3.3	0.0	90	4	2.21	
10549480	A2	9.75	8580	3.95	8900	4.6	-0.4		2	0.80	0.9579 ^c
10681464		11.48	8970	4.02	8900	4.5	-0.3		2	1.00	0.8599 ^b
HD 148542	A3IV	6.03	8470					92	6,7	2.04	

Table 2. Other stars observed spectroscopically. The columns are the same as in Table 1 except we have added a possible variability type in the last column.

KIC	Sp. type	Kp mag	T_{eff}^1 K	$\log g^1$ dex	T_{eff} K	$\log g$ dex	[Fe/H] dex	$v \sin i$ km s $^{-1}$	Ref	$\log \frac{L}{L_{\odot}}$	Period d	Type
3756846		15.75	11000	3.94						2.08		SPB
4281581		9.40	8290	3.84	8090	3.5	-0.1	113	1	1.93		δ Sct?
					8900	4.5	-0.3		2	1.00		
	A3IV-Vs				8200	3.9		105	3			
6462033		10.72	8530	4.32	18400	4.2	-0.3		2	3.00	0.6994 ^b	SPB
					7150	4.3		90	5			
7955898		12.32	8680	3.65	8300	3.7	-0.5		2	1.70	0.8132 ^b	δ Sct?
8324482	A0	11.61	8300	3.82	18900	4.2	-0.5		2	3.00		SPB
11152422		15.00	9290	4.02	9000	4.0	-1.4		2	1.40		δ Sct?

Stellar parameters determined from the low-dispersion HFOSC spectra have typical errors as follows: $T_{\text{eff}} = 300$ K, $\log g = 0.17$ dex, [Fe/H] = 0.13. Parameters from the MSS observations have the following typical errors: $T_{\text{eff}} = 250$ K, $\log g = 0.15$ dex, [Fe/H] = 0.1. These are certainly sufficient to locate a star in the H-R diagram with enough precision for our purposes. In addition to our spectroscopic results, Tables 1 and 2 also list spectroscopic parameters derived from the literature.

4 THE HOT γ DOR STARS

Most of the hot γ Dor star candidates listed in Table 1 are from Balona (2014). Also shown are additional candidates selected from *Kepler* γ Dor stars that are hotter than the granulation boundary. Antonello et al. (2006) discovered

line profile variations in HD 148542 (HR 6139) that can be explained by prograde g-modes similar to those observed in SPB stars, though it has a spectral type of A2V. This star can also be considered a candidate hot γ Dor variable.

HD 208727 was reported as an anomalous pulsator, but Kallinger et al. (2002) found it to be a rotational variable with a period of 0.317 d. Other candidates such as HD 29573 and γ CrB (Percy & Wilson 2000) are most likely rotational variables as well, but further observations are required.

The periodograms of the long-cadence (30-min exposures) of these stars and other stars are shown in Figs. 4 and 5. Note that in long-cadence data a frequency, ν , above 24 d^{-1} appears as a peak at approximately $(48 - \nu) \text{ d}^{-1}$. If the data were taken at strictly exact time intervals, it would not be possible to discern any frequencies higher than 24 d^{-1} . Fortunately this is not the case and it is indeed possible to identify frequencies higher than this value if the am-

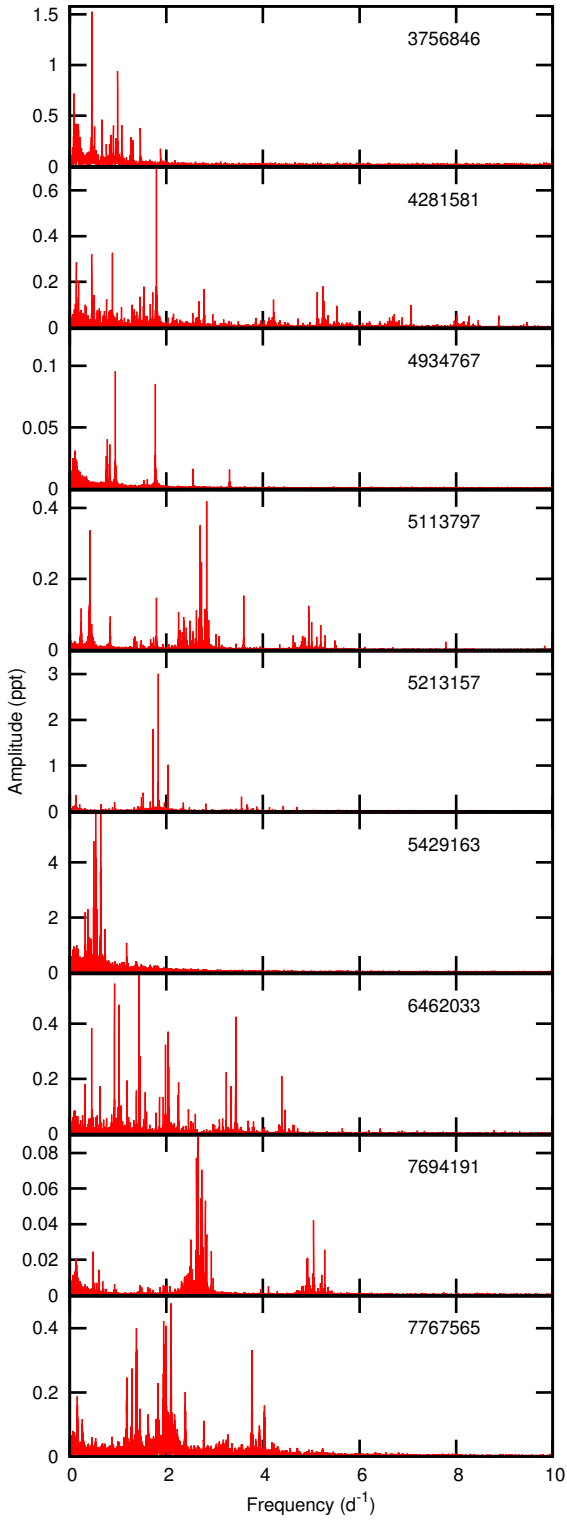


Figure 4. Periodograms of the hot γ Dor stars from KIC photometry. The stars are the anomalous hot γ Dor stars listed in Balona (2014).

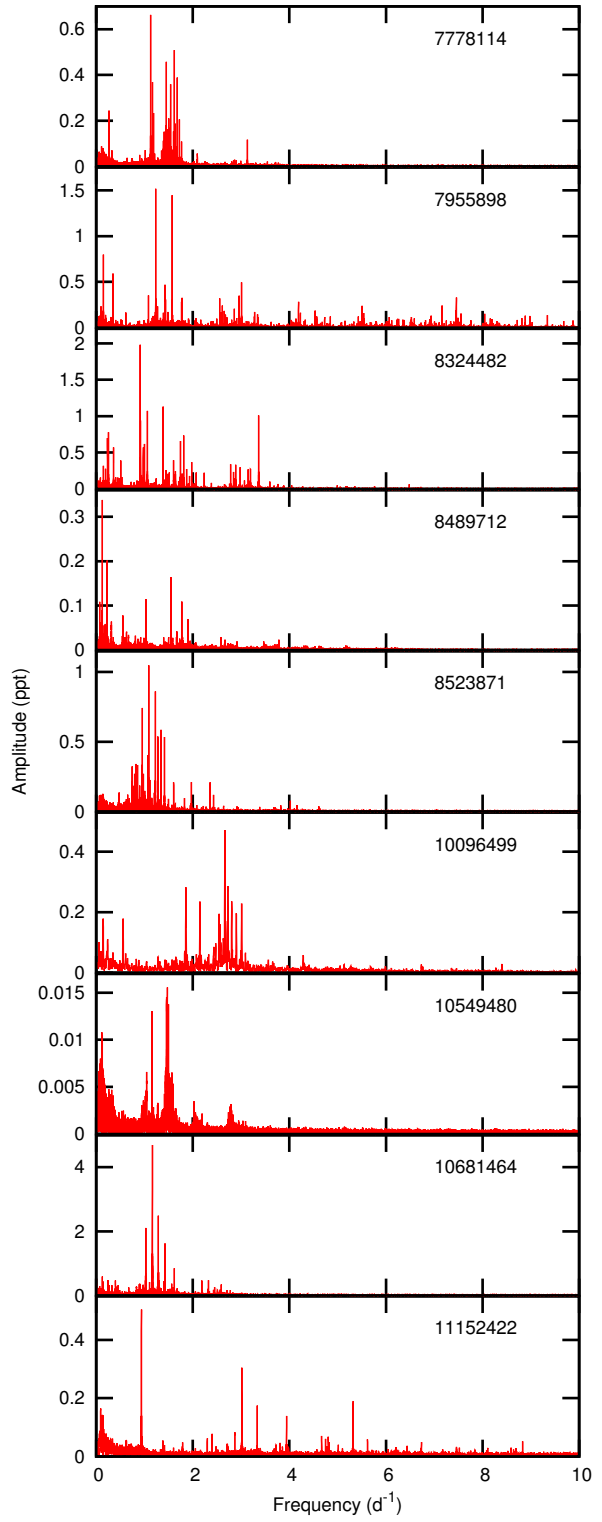


Figure 5. Periodograms of the hot γ Dor stars from KIC photometry. The stars are the anomalous hot γ Dor stars listed in Balona (2014).

plitudes are sufficiently high (Murphy et al. 2013). Examination of the long-cadence periodograms show that no such peaks are visible. Moreover, short-cadence data are available for KIC 5113797, 8489712 and 10549480 and it is clear that high frequencies are absent in these three stars.

In Table 2 we show stars which are probably SPB or δ Sct variables. KIC 4281581, KIC 7955898 and KIC 11152422 have some very low-amplitude peaks in the high-frequency range (Figs. 4, 5) and are possibly δ Sct variables. KIC 3756846, 6462033, 8324482 are hot enough to be classified as SPB stars.

For KIC 8489712 there is quite a large discrepancy between the $[\text{Fe}/\text{H}]$ value from Tkachenko et al. (2013) and from Niemczura et al. (2015). The difference in line strengths between the two abundance values is large, so either there is a mistake in one of these measurements or the star is a spectrum variable. Our measurements support the lower metallicity.

KIC 5113797, which is close to the open cluster NGC 6819, appears to show one flare (Balona 2015) and is also an X-ray source (Gosnell et al. 2012).

The largest discrepancy in Table 2 occurs for KIC 6462033 where we find $T_{\text{eff}} = 18400$ K, but Ulusoy et al. (2014) find $T_{\text{eff}} = 7150$ K. Our spectrum shows strong He I 4437 and He I 4471 which can only occur in a B star, so the difference is very puzzling. The field is slightly crowded, but KIC 6462033 is by far the brightest star in the field. The available photometry gives $B - V = -0.05$ which would also indicate a B star rather than a mid-A star.

The results in Table 1 mostly confirm that the stars are indeed significantly hotter than the blue edge of the known γ Dor stars. Using values of T_{eff} , $\log g$ and $[\text{Fe}/\text{H}]$, the luminosity may be estimated using the relationship in Torres et al. (2010). For those stars without spectroscopic estimates, we use the values listed in the KIC. The location of these stars in the theoretical H-R diagram is shown in Fig. 6. The red and blue edges of the γ Dor instability strips shown in this figure were both calculated using time-dependent theories of convection. In the calculations by Dupret et al. (2004), the location of the instability strip depends on the choice of mixing length parameter, α . Here we show the edges calculated with $\alpha = 2.0$ for modes with spherical harmonic $l = 1$. The strip moves towards cooler temperatures for smaller values of α . The red and blue edges calculated by Xiong et al. (2016) are for $l \leq 4$ and use a different non-local, time-dependent convection theory. The differences in location of the red and blue edges is quite remarkable and illustrates our poor understanding of convection and how it interacts with pulsation. As can be seen, the hot γ Dor stars are located outside the blue edge of the γ Dor instability strip and the red edge of the SPB instability strip.

5 MAIA VARIABLES

Reports of pulsating stars between the blue edge of the δ Sct instability strip and the red edge of the SPB instability strip have been reported from time to time. Struve (1955) suggested the possibility of a new class of variables on the basis of radial velocity observations of the late B star Maia, a member of the Pleiades. Later, Struve et al.

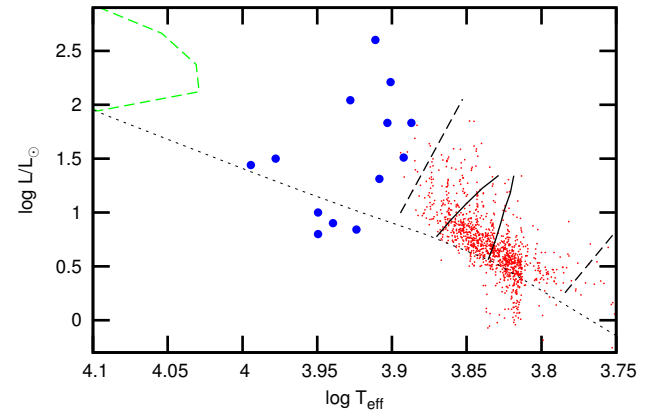


Figure 6. The location of the hot γ Dor variables in Table 1 in the theoretical H-R diagram is shown by large filled circles. The small (red) dots are normal γ Dor stars in the *Kepler* field. The dashed (green) region in the top left corner is the cool end of the SPB instability strip. The red and blue edges of the γ Dor instability strip calculated by Dupret et al. (2004) are shown as solid lines, while those calculated by Xiong et al. (2016) are shown by the dashed lines. The dotted line is the zero-age main sequence for solar composition (from Bertelli et al. 2008).

(1957) disclaimed such variability in Maia. Since that time, several attempts have been made to detect periodic variability in stars lying in this region of the H-R diagram, without success (McNamara 1985; Scholz et al. 1998; Lehmann et al. 1995). The situation is confusing because in these searches no distinction was made between high and low frequencies. Some variable stars lying in this region are probably best explained as rotational variables, as mentioned above.

Pulsation at high frequencies (i.e. higher than about 5 d^{-1}) are expected in the δ Sct stars but also among the β Cep variables. These are typically O9–B3 stars where the pulsations are driven by the ionization of metals of the iron group elements (Dziembowski & Pamiatnykh 1993). We define Maia variables as stars lying between the red edge of the β Cep instability strip and the blue edge of the δ Sct instability strip which show multiple high frequencies. Models indicate that such stars should not exist in this region.

One such star, α Dra, is classified as A0 III with a period of about 53 min and very small amplitude. This may be considered as a good example of a Maia variable (Kallinger et al. 2004). Degroote et al. (2009) and Balona et al. (2011b) found examples of B-type stars with high frequencies and low amplitudes which are significantly cooler than the red edge of the β Cep instability strip. These may also be considered as Maia candidates.

A list of Maia candidates compiled from the literature is given in Table 3. The atmospheric parameters of the presumed Maia variables observed by *CoRoT*, (CoRoT 102729531, 102771057, 102790063, 102861067, Degroote et al. 2009) were obtained from Strömgren photometry without the β index. Subsequently, spectroscopic observations have shown that these are mid-A stars (Sebastian et al. 2012). Therefore they are probably just normal δ Sct variables. Table 3 lists the five remaining *CoRoT* Maia candidates without spectral classifications. Better estimates of the stellar parameters are required to decide whether they are Maia variables or normal δ Sct stars.

Table 3. List of Maia star candidates. The spectral type and magnitude are shown together with estimates of the effective temperature, T_{eff} luminosity $\log L/L_{\odot}$, and projected rotational velocity. The last column shows the reference as follows: 1 - Prugniel et al. (2011); 2 - Balona et al. (2015a); 3 - Degroote et al. (2009); 4 - Aerts & Kolenberg (2005); 5 - Mowlavi et al. (2013); 6 - Lata et al. (2014).

Name	Sp. type	V mag	T_{eff} K	$\log \frac{L}{L_{\odot}}$	$v \sin i$ km s $^{-1}$	Ref
α Dra	A0III	3.68	10100	2.68	26	1
HD 121190	B9V		12200	1.96	118	4,5
HD 189637		10.86	19000	2.96		2
HD 234893	B5V	9.33	14700	2.87	130	2
HD 234999	B9	9.09	11150	2.08	103	2
HD 251584	B9	11.12				2
HD 253107	B1V	10.37	17600			2
CoRoT 102862454						3
CoRoT 102790331						3
CoRoT 102848985						3
CoRoT 102922479						3
CoRoT 102850576						3
CoRoT 102850502						3
KIC 2987640		12.64	11000	1.87		2
KIC 3343239		14.42	10691	1.97		2
KIC 3459297		12.55	10600	1.14		2
KIC 3756031	B5IV-V	10.00	16000	3.21	31	2
KIC 4939281		12.08	18900	3.08		2
KIC 8714886		10.95	19000	2.96		2
KIC 10285114		11.23	18200	2.74		2
KIC 11454304		12.95	17500	3.22		2
KIC 11973705	B8.5V/IV	9.12	11150	2.11	103	2
KIC 12258330	B5V	9.52	14700	2.88	130	2
EPIC 202061002	B9	12.40	9790	1.09		2
EPIC 202061129	B9	14.01	9600			2
EPIC 202061131	B5	14.23	14200			2
EPIC 202062129	B..	11.62	18000			2

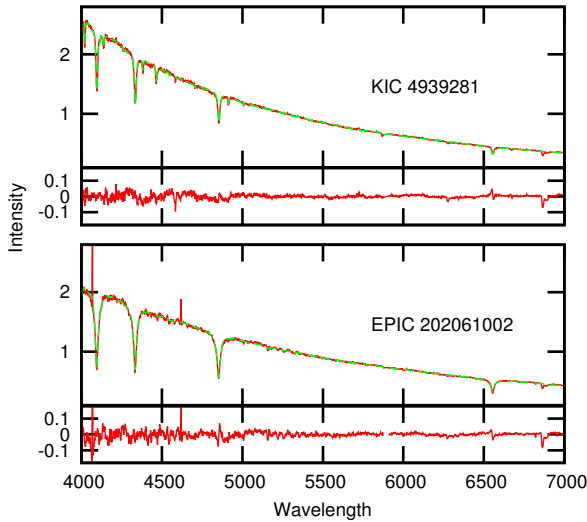


Figure 7. Observed and fitted spectra (top panel) and residuals (bottom panel) for two Maia candidates observed with HFOSC.

Estimation of atmospheric parameters in stars with spectral types between late B and early A is difficult. In this region the strength of the Balmer lines reaches a maximum. Since the effective temperature is estimated by fitting the $H\alpha$ or $H\beta$ line profiles, the value of T_{eff} is uncertain. For this reason, the discovery of possible Maia candidates in open clusters, such as NGC 3766 (Mowlavi et al. 2013) and

Table 3. Continued.

Name	Sp. type	V mag	T_{eff} K	$\log \frac{L}{L_{\odot}}$	$v \sin i$ km s $^{-1}$	Ref
NGC 3766-50		11.08	16600	3.04		5
NGC 3766-58		11.22	17200	2.96		5
NGC 3766-59		11.25	16500	2.95		5
NGC 3766-60		11.28	16500	2.93		5
NGC 3766-62		11.39	16500	2.87		5
NGC 3766-68		11.49	16300	2.81		5
NGC 3766-69		11.50	15600	2.80		5
NGC 3766-71		11.56	16600	2.77		5
NGC 3766-78		11.67	16500	2.70		5
NGC 3766-79		11.72	16000	2.67		5
NGC 3766-83		11.77	15800	2.64		5
NGC 3766-94		11.92	14600	2.55		5
NGC 3766-105		12.11	15500	2.43		5
NGC 3766-106		12.14	15800	2.42		5
NGC 3766-112		12.20	15600	2.38		5
NGC 3766-135		12.51	14500	2.19		5
NGC 3766-136		12.53	13300	2.18		5
NGC 3766-142		12.65	14700	2.10		5
NGC 3766-144		12.61	12200	2.10		5
NGC 3766-145		12.68	14200	2.09		5
NGC 3766-147		12.74	12900	2.04		5
NGC 3766-149		12.74	13700	2.05		5
NGC 3766-161		12.86	13800	1.97		5
NGC 3766-167		12.90	12900	1.95		5
NGC 3766-170		12.92	14000	1.93		5
NGC 3766-175		12.96	14000	1.91		5
NGC 3766-194		13.10	13200	1.82		5
NGC 3766-236		13.39	12300	1.65		5
NGC 3766-259		13.56	12000	1.54		5
NGC 3766-278		13.72	10300	1.45		5
NGC 1893-V60		14.53	9730	1.61		6
NGC 1893-V70		14.51	9700	1.61		6
NGC 1893-V71		14.44	12400	1.86		6
NGC 1893-V72		14.21	9900	1.75		6
NGC 1893-V74		14.22	10700	1.82		6
NGC 1893-V79		14.71	11400	1.67		6
NGC 1893-V81		14.17	12300	1.95		6
NGC 1893-V84		14.66	11500	1.75		6
NGC 1893-V89		14.24	11000	1.86		6
NGC 1893-V90		14.65	11200	1.73		6
NGC 1893-V91		14.56	12000	1.79		6
NGC 1893-V98		14.72	11000	1.64		6
NGC 1893-V102		14.38	9750	1.65		6
NGC 1893-V109		14.61	11700	1.75		6
NGC 1893-V123		14.45	9620	1.64		6
NGC 1893-V129		14.39	9620	1.63		6
NGC 1893-V145		13.97	11500	1.99		6

NGC 1893 (Lata et al. 2014), is very important because the position of the star along the main sequence is a much better indicator of T_{eff} .

We observed two Maia candidates, EPIC 202061002 and KIC 4939281 (Balona et al. 2015a) with the HFOSC. These spectra are shown in Fig. 7. For EPIC 202061002 the best fit gives $T_{\text{eff}} = 9790 \pm 340$, $\log g = 4.46 \pm 0.17$, $[\text{Fe}/\text{H}] = -1.7 \pm 0.1$. For KIC 4939281, $T_{\text{eff}} = 18900 \pm 660$, $\log g = 4.16 \pm 0.17$, $[\text{Fe}/\text{H}] = -0.4 \pm 0.1$. KIC 4939281 is just outside the β Cep instability strip and is perhaps better classified as a β Cep variable.

Mowlavi et al. (2013) divides the stars in NGC 3766 into five variability groups. The 13 stars in Group 1 are mostly monoprotic. Although they classified these stars as SPB variables, they may just as well be rotational variables. The 36 stars in Group 2 have periods in the range $0.1 < P < 1.1$ d. Of these, 23 stars are monoprotic, 11 biprotic and 2 have three frequencies. These stars fall between the SPB and δ Sct stars and are thus good candidates for Maia variables. However, the monoprotic stars with pe-

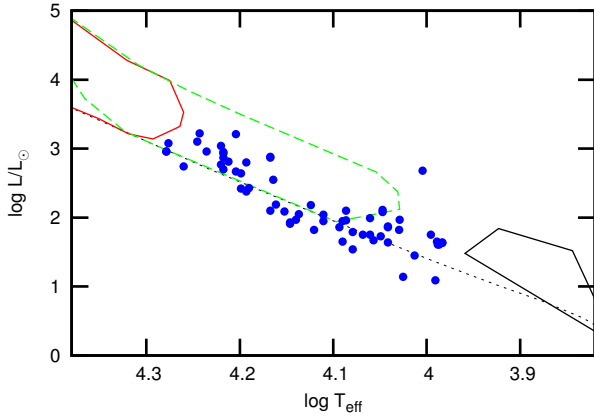


Figure 8. The location of Maia candidates (Table 3) in the theoretical H-R diagram. The three regions are the β Cep instability strip in the upper left corner (solid, red), the SPB instability strip (dashed, green) and the region populated by *Kepler* δ Sct stars in the lower right corner (solid, black). The dotted line is the zero-age main sequence.

riods longer than about 0.5 d can be considered as possible rotational variables. In Table 3 those stars which have periods too short to be due to rotation are listed. The other Groups consist of δ Sct and γ Dor stars.

We assume a distance modulus of $V_0 - M_V = 11.6 \pm 0.2$ mag and colour excess $E(B-V) = 0.22$ mag for NGC 3766 (McSwain et al. 2008). Given the apparent magnitude and assuming uniform reddening, we can determine the absolute magnitude, M_V . The observed main sequence is well-defined and represents an isochrone of about 2.5 Myr (McSwain et al. 2008). We can fit an isochrone of this age and solar abundance using the models in Bressan et al. (2012). From the isochrone we can derive T_{eff} as a function of colour index and $\log L/L_\odot$ from M_V . We used the bolometric correction as a function of T_{eff} by Torres (2010). The resulting values of T_{eff} and $\log L/L_\odot$ are shown in Table 3.

Among the 104 variables in NGC 1893 found by Lata et al. (2014), 17 stars could be classified as Maia variables on the basis of their locations in the H-R diagram and their short periods. These stars are listed in Table 3 with effective temperatures and luminosities taken from their paper. Except for a few stars with periods close to 0.5 d, the periods are too short to be due to rotation.

It should be noted that both Mowlavi et al. (2013) and Lata et al. (2014) provide no details regarding the significance of the detected periods or the alias structure. Results are presented in the form of phased light curves which, unfortunately, hides these details. It would have been far better to present the periodograms, which would enable a much more precise visual picture of the frequency structure and noise level in these data.

In Fig. 8 we show the location of the Maia candidates in the H-R diagram with respect to the β Cep, SPB and δ Sct instability strips. While it is possible that hotter stars may be re-classified as β Cep variables and the cooler stars as δ Sct variables, there still remains a considerable number of stars for which such a re-classification is unlikely. High-dispersion spectroscopic observations of these stars should clarify whether or not they are composite. In the meanwhile,

it is probable that a re-evaluation of the physics on which current models are based may be required.

6 DISCUSSION

It has been clear ever since the advent of high-precision photometry from space, that there is a serious problem with current models of pulsating stars in the upper main sequence. Models of δ Sct stars predict that only frequencies higher than about 5 d^{-1} are unstable, yet all δ Sct stars, when observed with sufficient precision, show unexplained multiple low frequencies (Balona 2014; Balona et al. 2015b). In addition, there is a growing realization that other types of pulsating stars exist in the upper main sequence, besides the δ Sct, β Cep and SPB variables. Furthermore, there is evidence that the atmospheres of A and B stars are more complex than previously thought. Here we refer to indications of superflares on A stars (Balona 2013) and starspots on both A and B stars (Balona 2016).

We need to remember that a large fraction of stars will show variability at the rotational frequency. In the past, the presence of spots or co-rotating features in upper main sequence stars has been thought unlikely because radiative envelopes cannot support a magnetic field. This view needs to be reconsidered in the light of the fact that nearly half of all A and B stars show what appears to be rotational modulation when observed with sufficient photometric precision (Balona 2013, 2016). Mis-classification of rotational modulation as pulsation certainly adds to the confusion.

In this paper we describe two types of anomalous pulsating stars. The hot γ Dor variables have multiple low frequencies, but no high frequencies, and lie between the red edge of the SPB and the blue edge of the γ Dor instability strip. The Maia variables have multiple high frequencies and lie between the red edge of the β Cep and the blue edge of the δ Sct instability strips. Current models are unable to account for pulsations in either of these two classes, adding to the problems of pulsation in the upper main sequence.

We observed several hot γ Dor candidates spectroscopically to verify their effective temperatures. In most cases the results confirm the anomalous nature of these objects. Two Maia candidates were also observed. These results, together with the anomalous cluster stars observed by Mowlavi et al. (2013) and Lata et al. (2014) and several well-observed brighter stars, leave little doubt that these two kinds of anomalous pulsating stars do exist.

One possible explanation for the hot γ Dor stars is that they are rapidly-rotating SPB stars, as suggested by Salmon et al. (2014) and Balona et al. (2015a). In a rapidly-rotating star, the equator is darker than the poles. If the star is observed equator-on, it will appear cooler than if it is observed pole-on. It is conceivable that such stars will appear to lie outside the red edge of the SPB instability strip and be seen as hot γ Dor variables. In that case, all hot γ Dor variables should have large projected rotational velocities, $v \sin i$. The mean $v \sin i$ for B5–B9 main sequence stars (the typical spectral type range of SPB variables) is $\langle v \sin i \rangle = 144 \text{ km s}^{-1}$ as derived from the catalogue of Glebocki & Gnacinski (2005). The mean value of the 6 stars in Table 1 with known projected rotational velocities is $\langle v \sin i \rangle = 114 \text{ km s}^{-1}$, which does not lend any support

to this idea. In any case, it is difficult to see how rotation can move the apparent location of an SPB star to a location near the hot end of the γ Dor instability strip, where most of these stars appear to lie (see Fig. 6). In fact, Salmon et al. (2014) found only a slight decrease in the apparent effective temperature of rotating stars as a result of gravity darkening.

A similar explanation could be proposed for the Maia variables, i.e. that they are rapidly-rotating β Cep stars observed nearly equator-on. The mean projected rotational velocity for O9–B3 main sequence stars (the typical spectral type range of β Cep variables) is $\langle v \sin i \rangle = 140 \text{ km s}^{-1}$ as derived from the catalogue of Glebocki & Gnacinski (2005). On the other hand, the mean value for the 7 stars in Table 3 is 92 km s^{-1} , which does not support this idea. Furthermore, it is difficult to understand how rotation can make a O9–B3 β Cep star to appear as an late B or early A star, as many Maia variables appear to be.

One can also assume that these stars are composite, which was proposed by Balona et al. (2011b). In the case of a hot γ Dor star the system would consist of a non-pulsating early A or B star and a cool γ Doradus companion. Because of the large luminosity difference, it would be difficult to detect the γ Dor companion in the composite spectrum. This possibility certainly should be investigated using high-dispersion, high signal-to-noise, spectroscopy. We found no evidence of a cool companion in any of the stars that were observed. A similar explanation can be proposed for Maia variables. In that case they need to be β Cep stars with a cool, though fairly luminous non-pulsating companion or else a δ Sct star with a B-type companion. This explanation does not seem plausible in the light of the numerous Maia candidates found in NGC 3766 (as many as 20 percent of the stars in the corresponding magnitude range, Mowlavi et al. 2013) and in NGC 1893 (Lata et al. 2014).

We conclude that the most probable explanation should be sought in a revision of opacities (Colgan et al. 2016; Moravveji 2016). In the light of the complexity of early-type atmospheres, a temperature inversion in the upper atmosphere may exist. In this case a modification of the outer boundary condition in pulsating models should perhaps be considered. Finally, it might be worth exploring the possibility of sub-surface convection zones in intermediate mass stars as was done by Cantiello et al. (2009) for massive stars.

ACKNOWLEDGMENTS

This work has been done under the Indo-South Africa project DST/INT/SA/P-02.

This paper includes data collected by the *Kepler* mission. Funding for the *Kepler* mission is provided by the NASA Science Mission directorate. The authors wish to thank the *Kepler* team for their generosity in allowing the data to be released and for their outstanding efforts which have made these results possible.

Much of the data presented in this paper were obtained from the Mikulski Archive for Space Telescopes (MAST). STScI is operated by the Association of Universities for Research in Astronomy, Inc., under NASA contract NAS5-26555. Support for MAST for non-HST data is provided by

the NASA Office of Space Science via grant NNX09AF08G and by other grants and contracts.

LAB wishes to thank the South African Astronomical Observatory and the National Research Foundation for financial support. SJ and ES acknowledges the grants INT/RFBR/P-118 and RFBR Grant No. 12-02-92693-IND-a jointly funded by DST Govt of India and Russian Academy of Science, Russia. Observations on the SAO RAS 6-meter telescope are carried out with financial support from the Ministry of Education and Science of the Russian Federation (agreement No. 14.619.21.0004, project ID RFMEFI61914X0004). ES is thankful to the Russian Science Foundation (grant No. 14-50-00043) for financial support of this study.

REFERENCES

- Aerts C., Kolenberg K., 2005, *A&A*, 431, 615
 Antonello E., Mantegazza L., Rainer M., Miglio A., 2006, *A&A*, 445, L15
 Balona L. A., 2013, *MNRAS*, 431, 2240
 —, 2014, *MNRAS*, 437, 1476
 —, 2015, *MNRAS*, 447, 2714
 —, 2016, *MNRAS*, 457, 3724
 Balona L. A., Baran A. S., Daszyńska-Daszkiewicz J., De Cat P., 2015a, *MNRAS*, 451, 1445
 Balona L. A., Daszyńska-Daszkiewicz J., Pamyatnykh A. A., 2015b, *MNRAS*, 452, 3073
 Balona L. A., Guzik J. A., Uytterhoeven K., Smith J. C., Tenenbaum P., Twicken J. D., 2011a, *MNRAS*, 415, 3531
 Balona L. A., Krisciunas K., Cousins A. W. J., 1994, *MNRAS*, 270, 905
 Balona L. A., Pigulski A., Cat P. D., Handler G., Gutiérrez-Soto J., Engelbrecht C. A., Frescura F., Briquet M., Cuypers J., Daszyńska-Daszkiewicz J., Degroote P., Dukes R. J., Garcia R. A., Green E. M., Heber U., Kawaler S. D., Lehmann H., Leroy B., Molenda-Zaaowicz J., Neiner C., Noels A., Nuspl J., Østensen R., Pricopi D., Roxburgh I., Salmon S., Smith M. A., Suárez J. C., Suran M., Szabó R., Uytterhoeven K., Christensen-Dalsgaard J., Kjeldsen H., Caldwell D. A., Girouard F. R., Sanderfer D. T., 2011b, *MNRAS*, 413, 2403
 Bertelli G., Girardi L., Marigo P., Nasi E., 2008, *A&A*, 484, 815
 Bradley P. A., Guzik J. A., Miles L. F., Uytterhoeven K., Jackiewicz J., Kinemuchi K., 2015, *AJ*, 149, 68
 Bressan A., Marigo P., Girardi L., Salasnich B., Dal Cero C., Rubele S., Nanni A., 2012, *MNRAS*, 427, 127
 Brown T. M., Latham D. W., Everett M. E., Esquerdo G. A., 2011, *AJ*, 142, 112
 Cantiello M., Langer N., Brott I., de Koter A., Shore S. N., Vink J. S., Voegler A., Lennon D. J., Yoon S., 2009, *A&A*, 499, 279
 Colgan J., Kilcrease D. P., Magee N. H., Sherrill M. E., Abdallah Jr. J., Hakel P., Fontes C. J., Guzik J. A., Mussack K. A., 2016, *ApJ*, 817, 116
 Cousins A. W. J., Warren P. R., 1963, *Monthly Notes of the Astronomical Society of South Africa*, 22, 65
 De Cat P., Eyer L., Cuypers J., Aerts C., Vandebussche B., Uytterhoeven K., Reyniers K., Kolenberg K., Groe-

- newegen M., Raskin G., Maas T., Jankov S., 2006, *A&A*, 449, 281
- Degroote P., Aerts C., Ollivier M., Miglio A., Debosscher J., Cuypers J., Briquet M., Montalbán J., Thoul A., Noels A., De Cat P., Balaguer-Núñez L., Maceroni C., Ribas I., Auvergne M., Baglin A., Deleuil M., Weiss W. W., Jorda L., Baudin F., Samadi R., 2009, *A&A*, 506, 471
- Dupret M., Grigahcène A., Garrido R., Gabriel M., Scuflaire R., 2004, *A&A*, 414, L17
- Dziembowski W. A., Pamiatnykh A. A., 1993, *MNRAS*, 262, 204
- Glebocki R., Gnacinski P., 2005, *VizieR Online Data Catalog*, 3244
- Gosnell N. M., Pooley D., Geller A. M., Kalirai J., Mathieu R. D., Frinchaboy P., Ramirez-Ruiz E., 2012, *ApJ*, 745, 57
- Guzik J. A., Kaye A. B., Bradley P. A., Cox A. N., Neuforge C., 2000, *ApJ*, 542, L57
- Handler G., 1999, *MNRAS*, 309, L19
- Henry G. W., Fekel F. C., 2005, *AJ*, 129, 2026
- Henry G. W., Fekel F. C., Henry S. M., 2005, *AJ*, 129, 2815
- Kallinger T., Iliev I., Lehmann H., Weiss W. W., 2004, in *IAU Symposium*, Vol. 224, *The A-Star Puzzle*, J. Zverko, J. Ziznovsky, S. J. Adelman, & W. W. Weiss, ed., pp. 848–852
- Kallinger T., Reegen P., Weiss W. W., 2002, *A&A*, 388, L37
- Koleva M., Prugniel P., Bouchard A., Wu Y., 2009, *A&A*, 501, 1269
- Lata S., Yadav R. K., Pandey A. K., Richichi A., Eswariah C., Kumar B., Kappelman N., Sharma S., 2014, *MNRAS*, 442, 273
- Lehmann H., Scholz G., Hildebrandt G., Klose S., Panov K. P., Reimann H.-G., Woche M., Ziener R., 1995, *A&A*, 300, 783
- McDonald I., Zijlstra A. A., Boyer M. L., 2012, *MNRAS*, 427, 343
- McNamara B. J., 1985, *ApJ*, 289, 213
- McSwain M. V., Huang W., Gies D. R., Grundstrom E. D., Townsend R. H. D., 2008, *ApJ*, 672, 590
- Moravveji E., 2016, *MNRAS*, 455, L67
- Mowlavi N., Barblan F., Saesen S., Eyer L., 2013, *A&A*, 554, A108
- Murphy S. J., Shibahashi H., Kurtz D. W., 2013, *MNRAS*, 430, 2986
- Nielsen M. B., Gizon L., Schunker H., Karoff C., 2013, *A&A*, 557, L10
- Niemczura E., Murphy S. J., Smalley B., Uytterhoeven K., Pigulski A., Lehmann H., Bowman D. M., Catanzaro G., van Aarle E., Bloemen S., Briquet M., De Cat P., Drobek D., Eyer L., Gameiro J. F. S., Gorlova N., Kamiński K., Lampens P., Marcos-Arenal P., Pápics P. I., Vandebussche B., Van Winckel H., Stešlicki M., Fagas M., 2015, *MNRAS*, 450, 2764
- Pamyatnykh A. A., 2000, in *Astronomical Society of the Pacific Conference Series*, Vol. 210, *Delta Scuti and Related Stars*, Breger M., Montgomery M., eds., p. 215
- Percy J. R., Wilson J. B., 2000, *PASP*, 112, 846
- Prugniel P., Vauglin I., Koleva M., 2011, *A&A*, 531, A165
- Reinhold T., Reiners A., Basri G., 2013, *A&A*, 560, A4
- Salmon S. J. A. J., Montalbán J., Reese D. R., Dupret M.-A., Eggenberger P., 2014, *A&A*, 569, A18
- Sánchez-Blázquez P., Peletier R. F., Jiménez-Vicente J., Cardiel N., Cenarro A. J., Falcón-Barroso J., Gorgas J., Selam S., Vazdekis A., 2006, *MNRAS*, 371, 703
- Scholz G., Lehmann H., Hildebrandt G., Panov K., Iliev L., 1998, *A&A*, 337, 447
- Sebastian D., Guenther E. W., Schaffenroth V., Gandolfi D., Geier S., Heber U., Deleuil M., Moutou C., 2012, *A&A*, 541, A34
- Strassmeier K. G., 2009, *A&A Rev.*, 17, 251
- Struve O., 1955, *S&T*, 14, 461
- Struve O., Sahade J., Lynds C. R., Huang S. S., 1957, *ApJ*, 125, 115
- Tkachenko A., Lehmann H., Smalley B., Uytterhoeven K., 2013, *MNRAS*, 431, 3685
- Torres G., 2010, *AJ*, 140, 1158
- Torres G., Andersen J., Giménez A., 2010, *A&A Rev.*, 18, 67
- Ulusoy C., Stateva I., Iliev I. K., Ulaş B., 2014, *New Astronomy*, 30, 28
- Valenti J. A., Piskunov N., 1996, *A&AS*, 118, 595
- Xiong D. R., Deng L., Zhang C., Wang K., 2016, *MNRAS*, 457, 3163